

# Heat transfer in ground heat exchangers with groundwater advection

Nairen Diao<sup>a</sup>, Qinyun Li<sup>b</sup>, Zhaohong Fang<sup>b,\*</sup>

<sup>a</sup> Department of Engineering Mechanics, Tsinghua University, Beijing 100084, China

<sup>b</sup> The Ground Source Heat Pump Research Center, Shandong Institute of Architecture and Engineering, Jinan 250014, China

Received 17 June 2003; received in revised form 29 March 2004; accepted 6 April 2004

Available online 20 July 2004

## Abstract

In order to estimate the impact of groundwater flow on performance of geothermal heat exchangers in ground source heat pump systems, an equation of conduction–advection is established for heat transfer in porous media, and an analytical transient solution is obtained for a line heat source in an infinite medium by means of the Green function analysis. An explicit expression has also been derived of the mean temperature on circles around the heat source. Dimensionless criteria that dictate the process are summarized, and influence of the groundwater advection on the heat transfer is discussed accordingly. Computations show that water advection in the porous medium may alter significantly the conductive temperature distribution, result in lower temperature rises and lead to a steady condition eventually. The hydraulic and thermal properties of soils and rocks influencing the advection heat transfer are briefly summarized. The analytical solution has provided a theoretical basis and practical tool for design and performance simulation of the ground heat exchangers.

© 2004 Elsevier SAS. All rights reserved.

**Keywords:** Heat transfer; Conduction; Advection; Porous medium; Ground source heat pump; Ground heat exchanger

## 1. Introduction

Ground-coupled heat pump (GCHP) systems are increasingly deployed for heating and air-conditioning in commercial and institutional buildings as well as in residential ones [1,2]. These systems consist of a sealed loop of pipe, buried in the ground and connected to a heat pump through which water/antifreeze is circulated. For the ground-loop heat exchangers, vertical borehole configuration is usually preferred over horizontal trench systems because less ground areas are required. The vertical ground heat exchanger (GHE) consists of a number of boreholes, each containing a U-tube pipe. The depth of the borehole ranges usually between 40–150 m, and the diameter 0.075–0.15 m. The borehole annulus should be grouted with materials that provide thermal contact between the pipe and the surrounding soil/rock and to protect groundwater from possible contamination. The efficiency of GCHP systems are inherently higher than that of air source heat pumps because the ground maintains a relatively stable source/sink temperature, allowing

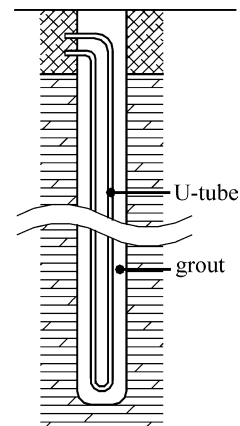


Fig. 1. Schematic diagram of a vertical borehole GHE.

the heat pump to operate close to its optimal design point. The schematic diagram of a borehole is shown in Fig. 1.

Although low operating and maintenance costs mean that these systems generally have attractive life-cycle costs, the construction costs of the GHEs are critical for the economical competitiveness of GCHP systems in the heating and air-conditioning market. It is important to work out analytical tools by which the thermal behavior of any GCHP

\* Corresponding author. Fax: 86-531-6952404.

E-mail addresses: [dnrw@jn-public.sd.cninfo.net](mailto:dnrw@jn-public.sd.cninfo.net) (N. Diao), [lqy@sdaie.edu.cn](mailto:lqy@sdaie.edu.cn) (Q. Li), [fangzh@sdaie.edu.cn](mailto:fangzh@sdaie.edu.cn) (Z. Fang).

### Nomenclature

|       |   |   |                      |   |                                 |
|-------|---|---|----------------------|---|---------------------------------|
| $a$   | thermal diffusivity . . . . .                                   | $\text{m}^2 \cdot \text{s}^{-1}$                    | $x$                  | coordinate . . . . .                                | $\text{m}$                      |
| $c$   | specific heat . . . . .   | $\text{J} \cdot \text{kg}^{-1} \cdot \text{K}^{-1}$ | $y$                  | coordinate . . . . .                                | $\text{m}$                      |
| $Fo$  | $= U^2 \tau / a$ , non-dimensional time                         |   | <i>Greek symbols</i> |   |                                 |
| $h$   | hydraulic head . . . . .  | $\text{m}$  | $\varepsilon$        | porosity  |                                 |
| $k$   | thermal conductivity . . . . .                                  | $\text{W} \cdot \text{m}^{-1} \cdot \text{K}^{-1}$  | $\eta$               | integration parameter                               |                                 |
| $K$   | hydraulic conductivity . . . . .                                | $\text{m} \cdot \text{s}^{-1}$                      | $\rho$               | density . . . . .                                   | $\text{kg} \cdot \text{m}^{-3}$ |
| $L$   | $= k / (u \rho_w c_w)$ , characteristic length . . . . .        | $\text{m}$  | $\theta$             | $= t - t_0$ , temperature rise . . . . .            | $\text{K}$                      |
| $N$   | number of boreholes in GHE field                                |   | $\Theta$             | $= 2\pi k \theta / q_l$ , dimensionless temperature |                                 |
| $q$   | volumetric flow rate . . . . .                                  | $\text{m} \cdot \text{s}^{-1}$                      | $\varphi$            | polar angle   |                                 |
| $q_l$ | heat flow per unit length of the line source . . . . .          | $\text{W} \cdot \text{m}^{-1}$                      | $\tau$               | time . . . . .                                      | $\text{s}$                      |
| $r$   | radial coordinate . . . . .                                     | $\text{m}$  | <i>Subscripts</i>    |   |                                 |
| $r_b$ | borehole radius . . . . .                                       | $\text{m}$  | 0                    | without advection                                   |                                 |
| $R$   | $= Ur/a$ , non-dimensional coordinate                           |   | $m$                  | multiple borehole                                   |                                 |
| $t$   | temperature . . . . .   | $\text{K}$  | $s$                  | solid, steady                                       |                                 |
| $t_0$ | initial temperature . . . . .                                   | $\text{K}$  | $w$                  | water   |                                 |
| $T$   | $= k \rho c / (u \rho_w c_w)^2$ , characteristic time . . . . . | $\text{s}$  | <i>Superscript</i>   |   |                                 |
| $u$   | advection velocity . . . . .                                    | $\text{m} \cdot \text{s}^{-1}$                      | –                    | average   |                                 |
| $U$   | $= u \rho_w c_w / (\rho c)$ , revised velocity . . . . .        | $\text{m} \cdot \text{s}^{-1}$                      |                      |   |                                 |

system can be assessed and then, optimized in technical and economical aspects.

In practice, the boreholes of GHEs may penetrate several geologic strata. The ability of the vertical borehole exchanger to exchange heat with the ground depends on local geology, hydrogeology and other conditions that impact the feasibility and economics of the GCHP systems. Heat transfer between a GHE and its surrounding soil/rock is rather complicated and difficult to model for the purpose of sizing the exchanger or energy analysis of the system. Besides the structural and geometrical configuration of the exchanger a lot of factors influence the exchanger performance, such as the ground temperature distribution, soil moisture content and its thermal properties, groundwater movement and possible freezing and thawing in soil. The heat dissipation from the pipes in boreholes to far-field ground is a transient process involving a large domain and complicated geometry. The presence of groundwater makes the heat transfer process even more intricate. Water movement in actual “streams” in underground channels is rare and confined to specific geological situations. The subsurface, however, generally has porosity (voids and fractures). The water table is the dividing line between ground with some air in the pores and ground that is saturated with water. Below that level, water is held and moves between the grains of geologic formations in response to hydraulic gradients. Rates of lateral groundwater flow vary, ranging from meter per year to meters per day according to local geologic and hydraulic conditions. High flow rates will generally be associated with specific strata types, particularly very coarse gravels or sands. Thus, the heat dissipation in aquifers may be regarded as a coupled

process of heat conduction through the solid matrix and water in its pores and heat advection by moving groundwater.

One of the primary objectives in the design of reliable GCHP systems is properly sizing the ground heat exchanger. A lot of efforts have been made to understand and formulate the heat transfer process in the GHEs. On this basis a few tools are commercially available for design and/or performance simulation of the GHEs with varying sophistications [3–7]. All of the design tools, however, are based simply on principles of heat conduction, and do not consider the implications of groundwater flow in carrying away heat. The reasons for such simplification are the difficulties encountered both in modeling and computing the convective heat transfer and in learning about the actual groundwater flow in engineering practice. As a consequence, the effect of the groundwater advection is usually assumed negligible in GHE designs so far.

In general, groundwater flow is beneficial to the thermal performance of GHEs since it has a moderating effect on borehole temperatures in both heating and cooling modes. Besides, the thermal load of commercial and institutional buildings is often dominated by cooling requirement that means the system rejects more heat into the ground than it extracts from it. For building in cold climate, a much larger heating load may also occur, then, a net heat extraction may be accumulated in the lifetime operation of the system. According to the sheer conduction model the required ground-loop heat exchanger lengths are significantly greater than the required lengths if the annual load were balanced so as to adequately dissipate the imbalanced annual loads. On the other hand, a moderate groundwater advection is expected to make notable difference in alleviating the

possible heat buildup around the borehole over time. As a result, it is desirable to account for the groundwater flow in the heat transfer model to avoid over-sizing of the ground heat exchangers.

Among the few reports on the effect of the groundwater flow found in literature Eskilson [8] has discussed the problem based on a steady-state analytical solution given by Carslaw and Jeager [9]. Because the heat dissipation in the GHEs with or without water advection is characterized as a transient process covering a long duration, the steady-state analysis provides only limited understandings of the groundwater advection impacts. Chiasson et al. [10] have made a preliminary investigation of the effects of groundwater flow on the heat transfer of vertical borehole heat exchangers and the ability of current design and in-situ thermal conductivity measurement techniques to deal with these effects. A finite element numerical model was used in solving the transient two-dimensional combined heat transfer. Thermal performances of a single borehole and a 4 × 4 borehole field were simulated in various geological conditions. No general conclusions and correlations among the influencing parameters were obtained due to the discrete nature of the approach.

The work reported here tries to study the combined heat transfer of conduction and advection in the vertical borehole heat exchangers by an analytical approach. A two-dimensional model similar to Chiasson’s has been solved analytically, and an explicit expression of the temperature response has been derived describing correlation among various factors, which have impacts on this process. The analytical solution results in some dimensionless parameters, facilitates both qualitative and quantitative analyses of the process. Besides, the analytical expression can be readily integrated into existing models and software for design and performance simulation of vertical GHEs since it is much more convenient for computation than any numerical solutions of the problem.

## 2. Formulation and solution of combined heat transfer

### 2.1. The energy equation for porous media with water advection

As mentioned above, heat transfer in GHEs is complicated and dependent of multiple factors, some of which are hard to grasp accurately in engineering practice. It is inevitable to make assumptions and simplifications in the study so that impacts of certain factors can be highlighted and analyzed in detail. In following discussions the ground around the boreholes is assumed to be a homogeneous porous medium saturated by groundwater.

Liquid flow in a porous medium is usually described by Darcy’s law, which can be expressed as

$$q = -K \frac{dh}{dx} \quad (1)$$

where  $K$  is the hydraulic conductivity, and  $h$  the hydraulic head. The volumetric flow rate per unit of cross-sectional area,  $q$ , is equal to the average linear velocity of the liquid over the cross-section.

Heat is transported through a saturated porous medium in a combined mechanism: by conduction through its solid matrix and liquid in its pores as well as by convection of the moving liquid. By applying the law of conservation of energy to a control volume, an equation for heat transfer in the saturated porous medium can be expressed as:

$$\rho c \frac{\partial t}{\partial \tau} + \rho_w c_w \vec{V} \cdot \nabla t = \nabla \cdot (k \nabla t) \quad (2)$$

where  $k$  denotes the effective thermal conductivity of the porous medium;  $\rho c$  is the volumetric specific heat of the porous medium, including both the solid matrix and water in its pores, and  $\rho_w c_w$  the volumetric specific heat of water. Note in the equation that heat is stored and conducted through both the water and soil matrix, but only water takes part in convection of heat here. The average linear groundwater velocity  $\vec{V}$  over a cross-section of the medium may be determined by the hydraulic head distribution according to the Darcy’s law if the hydraulic conductivity of the medium is known.

The effective thermal conductivity and the volumetric specific heat of the porous medium are weighted averages of those of the saturated water and solid matrix, and can usually be determined on basis of its porosity  $\varepsilon$  as

$$\begin{cases} k = \varepsilon k_w + (1 - \varepsilon) k_s \\ \rho c = \varepsilon \rho_w c_w + (1 - \varepsilon) \rho_s c_s \end{cases} \quad (3)$$

Following the Eskilson’s model [8], a further approximation is accepted that the groundwater velocity is uniform in the whole domain concerned and parallel to the ground surface. The term “advection” is often used to describe such a flow. Define the velocity  $u$  is in the direction of the  $x$ -coordinate. Then, on the assumption of constant thermal properties Eq. (2) reduces to

$$\frac{\partial t}{\partial \tau} + U \frac{\partial t}{\partial x} = a \nabla^2 t \quad (4)$$

where  $U = u \rho_w c_w / (\rho c)$ , and the effective thermal diffusivity  $a = k / (\rho c)$ .

And for the steady-state situations Eskilson studied, the heat transfer equation is further simplified to

$$U \frac{\partial t}{\partial x} = a \nabla^2 t \quad (5)$$

### 2.2. Solution of the line source problem with water advection

In order to discuss the effect of groundwater advection on heat transfer of the borehole heat exchangers the authors have derived an analytical solution of the transient problem under following assumptions:

- (1) The ground is regarded as homogeneous and semi-infinite medium, and its physical properties do not change with temperature;
- (2) The effects of the ground surface as a boundary and the finite length of the borehole are neglected. Then, the problem may be simplified as two-dimensional;
- (3) As commonly accepted in models for heat transfer in vertical GHEs, the borehole is approximated by a line heat source while determining the temperature rise on the borehole wall and beyond;
- (4) The medium has a uniform initial temperature,  $t_0$ ;
- (5) As a basic case of study, the heating rate per length of the source,  $q_1$ , is constant since a starting instant,  $\tau = 0$ .

Eq. (4) of conduction–advection is the same in mathematical formulation as the conduction equation with a moving heat source when the equivalent velocity  $U$  is used in the place of the moving speed of the heat source. The studies on conduction with moving heat sources deal with either problems in which heat sources move through a fixed medium, or cases of fixed heat sources past that a uniformly moving medium flows. Some monographs [9,11] on heat transfer have discussed such problems, and presented the solution of a moving line source on steady conditions. Following the same approach, the authors have derived the solution on transient conditions [12]. When a single line source is deployed at the origin of the coordinates, the temperature rise in the medium,  $\theta = t - t_0$ , of the discussed case can be obtained simply by means of the Green's function method, and written as

$$\theta(x, y, \tau) = \frac{q_1}{4\pi k} \int_0^\tau \frac{1}{(\tau - \tau')} \times \exp\left[-\frac{[x - U(\tau - \tau')]^2 + y^2}{4a(\tau - \tau')}\right] d\tau' \quad (6)$$

Introducing a new parameter,  $\eta = 4a(\tau - \tau')/r^2$ , in the place of  $\tau'$ , for the integration, we obtain

$$\theta(x, y, \tau) = \frac{q_1}{4\pi k} \exp\left(\frac{Ux}{2a}\right) \int_0^{r^2/(4a\tau)} \frac{1}{\eta} \times \exp\left[-\frac{1}{\eta} - \frac{U^2 r^2 \eta}{16a^2}\right] d\eta \quad (7)$$

where  $r = \sqrt{x^2 + y^2}$ . Or in the polar coordinates it takes the form

$$\theta(r, \varphi, \tau) = \frac{q_1}{4\pi k} \exp\left(\frac{Ur}{2a} \cos \varphi\right) \int_0^{r^2/(4a\tau)} \frac{1}{\eta} \times \exp\left[-\frac{1}{\eta} - \frac{U^2 r^2 \eta}{16a^2}\right] d\eta \quad (8)$$

Eq. (7) reduces to the solution of the steady condition while the time approaches infinity, that is

$$\theta_s(x, y) = \frac{q_1}{2\pi k} \exp\left(\frac{Ux}{2a}\right) K_0\left[\frac{Ur}{2a}\right] \quad (9)$$

where  $K_0(z)$  is the modified Bessel function of the second kind of order zero.

On the other hand, for the specific instance when the advection velocity  $u$  and, then  $U = u\rho_w c_w/(\rho c)$ , is zero, Eq. (7) reduces to the common temperature response of the line source in an infinite medium:

$$\theta_0(r, \tau) = -\frac{q_1}{4\pi k} Ei\left(-\frac{r^2}{4a\tau}\right) \quad (10)$$

where  $Ei(z)$  is the exponential integral function. As this expression indicates, the temperature in the medium will keep rising and no steady condition will be reached when the time lasts to infinity.

Select  $L = \frac{a}{U} = \frac{k}{u\rho_w c_w}$  as a characteristic length, and  $T = \frac{a}{U^2} = \frac{k\rho c}{(u\rho_w c_w)^2}$  as a characteristic time of the problem. We define the non-dimensional temperature excess  $\Theta = \frac{2\pi k \theta}{q_1}$ , the non-dimensional radial coordinate  $R = \frac{r}{L} = \frac{Ur}{a}$  and non-dimensional time  $Fo = \frac{\tau}{T} = \frac{U^2 \tau}{a}$ . Another dimensionless parameter involved is the polar angle,  $\varphi$ . Thus, Eq. (8) can be rewritten in a dimensionless form as

$$\Theta(R, \varphi, Fo) = \exp\left(\frac{R \cos \varphi}{2}\right) \int_0^{R^2/(4Fo)} \frac{1}{2\eta} \times \exp\left[-\frac{1}{\eta} - \frac{R^2 \eta}{16}\right] d\eta \quad (11)$$

The non-dimensional temperature distribution on steady conditions is independent of time, which results in

$$\Theta_s = \exp\left(\frac{R \cos \varphi}{2}\right) K_0\left[\frac{R}{2}\right] \quad (12)$$

### 3. Computation and discussion

The temperature responses of above equations can be computed readily by appropriate integration schemes, which take much less computing time and assures more reliable precision than numerical solutions of the governing equation by the finite element or finite difference methods.

#### 3.1. Temperature isotherms

Eq. (10) indicates that the temperature response to the line source heating is symmetric about the origin in a medium without advection. When the water advection plays a role in the heat transfer, the temperature distributions become two-dimensional with a downstream bias of the temperature rise. Isotherms at different instants are shown in Fig. 2.

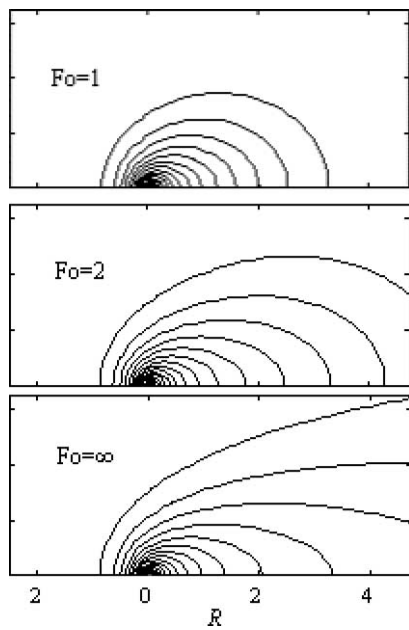


Fig. 2. Isotherms of a line-source in an infinite medium with water advection.

### 3.2. Temperature variation around a circle and the mean temperature on it

The temperatures on a circle around the heat source are no longer identical due to the heat carried downstream by water advection. It is desirable sometimes to know the mean temperature on such circles, for example, the borehole wall. The mean temperature can be defined as an integral average on the circle, which turns out to be

$$\begin{aligned} \bar{\Theta}(R, Fo) &= \frac{1}{\pi} \int_0^\pi \Theta(R, \varphi, Fo) d\varphi \\ &= I_0\left(\frac{R}{2}\right) \int_0^{R^2/(4Fo)} \frac{1}{2\eta} \exp\left[-\frac{1}{\eta} - \frac{R^2\eta}{16}\right] d\eta \end{aligned} \quad (13)$$

according to an correlation about  $I_0(z)$ , the modified Bessel function of the first kind of order zero:

$$\frac{1}{\pi} \int_0^\pi \exp[z \cos \varphi] d\varphi = \sum_{m=0}^\infty \frac{z^{2m}}{2^{2m}(m!)^2} = I_0(z)$$

Comparison between Eqs. (11) and (13) shows that the ratio of the temperature rise at a certain location to the mean value on the circle at the same distance from the source is independent of time, that is

$$\frac{\Theta(R, \varphi, Fo)}{\bar{\Theta}(R, Fo)} = \frac{\exp\left(\frac{R}{2} \cos \varphi\right)}{I_0\left(\frac{R}{2}\right)} \quad (14)$$

Results from Eq. (14) are plotted in Fig. 3, showing variations in the temperature rise along the circle. It is clear that the temperature rise in the downstream direction ( $\varphi = 0$ )

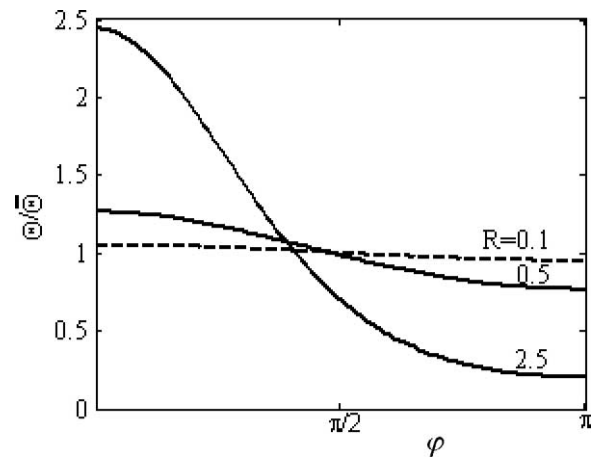


Fig. 3. The temperature rise on a circle around the heat source.

is higher than that in the upstream direction ( $\varphi = \pi$ ) due to the heat transfer by advection. It can also be seen that the difference in the temperature around the circle diminishes with decrease in  $R$ . Calculations indicate that the ratio  $\Theta/\bar{\Theta}$  is restricted between 0.99 and 1.01 as long as  $R$  is less than 0.005. In this sense the non-dimensional parameter  $R$ , which is proportional to the advection velocity, may serve as a quantitative index in characterizing the impact of the groundwater advection; and  $R < 0.005$  is recommended to be a criterion that the impact of water advection on the heat transfer may be neglected.

### 3.3. Temperature response over time

The temperature responses are computed according to Eqs. (10) and (11) and plotted in Fig. 4 against the dimensionless parameter  $Fo/R^2 = a\tau/r^2$  so as to facilitate comparison between the models with and without advection.

It is noticeable that the dimensionless parameter  $R$ , which may be used to characterize the effect of groundwater advection, makes significant difference in the temperature responses. The temperature responses at upstream and downstream locations also differ notably especially when  $R$  is large enough, say,  $R > 0.1$ . The temperatures at downstream locations ( $\varphi = 0$ ) rise above that of the reference case of pure conduction ( $R = 0$ ) at the early stage of the response, but later drop below the reference temperature and finally turn to steady temperatures.

### 3.4. The time to reach the steady state

It is one of the prominent features of the heat transfer of the line source with advection that its temperature response tends to steady conditions in contrast to the continuous increase to infinity in the reference case where no water flow exists. Although it takes infinitely long time for the temperature at certain locations to reach the steady condition in the mathematical sense, it is desirable to define a nominal duration to reach the steady state for the purpose of

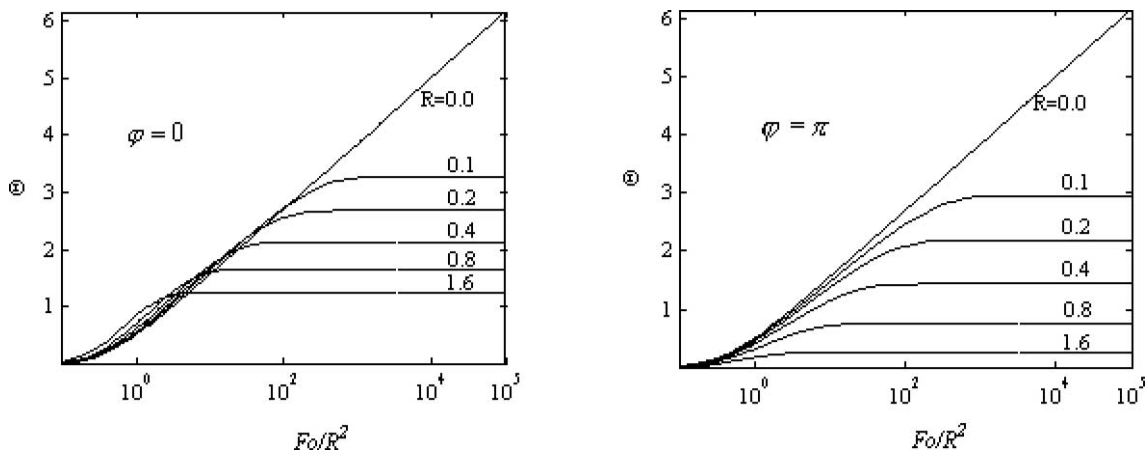


Fig. 4. Temperature responses to the line-source heating with and without water advection.

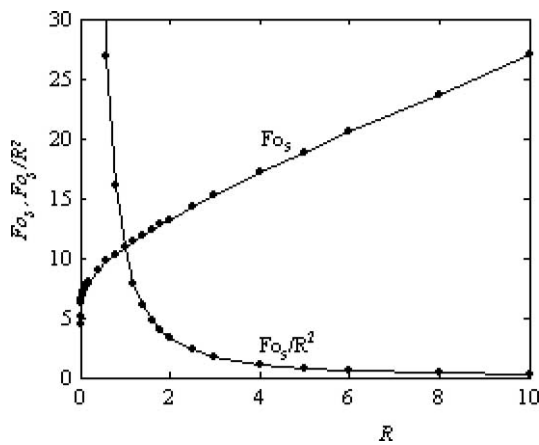


Fig. 5. The dimensionless time to reach the steady state.

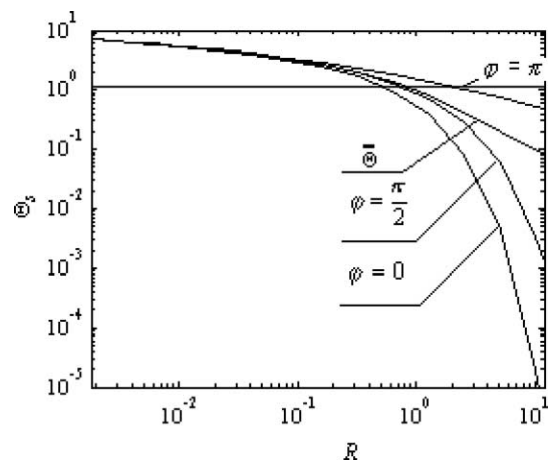


Fig. 6. The temperature excess on the steady conditions.

practical applications. The nominal steady state at a certain location may be regarded to have been established when its temperature excess reaches 0.99 of that of the steady state. According to this definition the nominal duration to reach the steady condition,  $\tau_s$ , is figured out according to Eqs. (11) and (12). Both the dimensional parameters  $Fo_s$  and  $Fo_s/R^2$  are shown against  $R$  in Fig. 5. Notice that  $Fo_s = \frac{\tau_s}{T} = \frac{(u\rho_w c_w)^2 \tau_s}{k\rho c}$  is independent of  $r$ , so the curve of  $Fo_s$  versus  $R$  reflects the change in  $\tau_s$  with the horizontal distance  $r$ .  $Fo_s$  approaches about 4, as  $R$  tends to zero. It can be seen that  $Fo_s$  increases gently with  $R$ . This means that the horizontal distance from the heat source make minor difference in  $\tau_s$ . On the other hand, because  $Fo_s/R^2 = a\tau_s/r^2$  is independent of the advection velocity  $u$ , and  $R = u\rho_w c_w r/k$  is proportional to  $u$ , the curve of  $Fo_s/R^2$  versus  $R$  indicates the change in  $\tau_s$  with  $u$ . The curve shows that  $Fo_s/R^2$  tends to infinity when  $R$ , i.e.,  $u$ , approaches zero; and  $Fo_s/R^2$  decreases sharply with increase in  $R$ . This means the advection velocity  $u$  has a strong impact on the duration to reach the steady condition. Owing to the fact that  $Fo_s$  is within a limited range of about 4 to 27 as  $R < 10$ , which is of the greatest significance in the GHE applications, the duration to reach the steady condition

$\tau_s = Fo_s \cdot T$  can be estimated according to the characteristic time  $T$  of particular cases. The characteristic time of various geological formations will be discussed in the following section.

The temperature excesses on the steady conditions are shown in Fig. 6. It can be seen again that the steady temperature excesses at locations with the same distance  $r$  but different angle  $\varphi$  differ little as long as  $R < 0.1$ . Besides, the steady temperature excesses diminish sharply with increase in  $R$  when  $R$  exceeds unity.

### 3.5. Borehole field and variable heating rate

Multi-borehole GHEs are more commonly employed in practical applications of the ground source heat pump systems. The heat transfer process of a single borehole in the GHE discussed above has provided a foundation for analysis of borehole fields comprising multiple boreholes in arbitrary configurations. The temperature excess at any location in a field with multiple boreholes may be obtained by means of the superimposition principle owing to the linearity of the problem defined. Generally, for a ground heat exchanger composed of  $N$  boreholes the temperature rise on

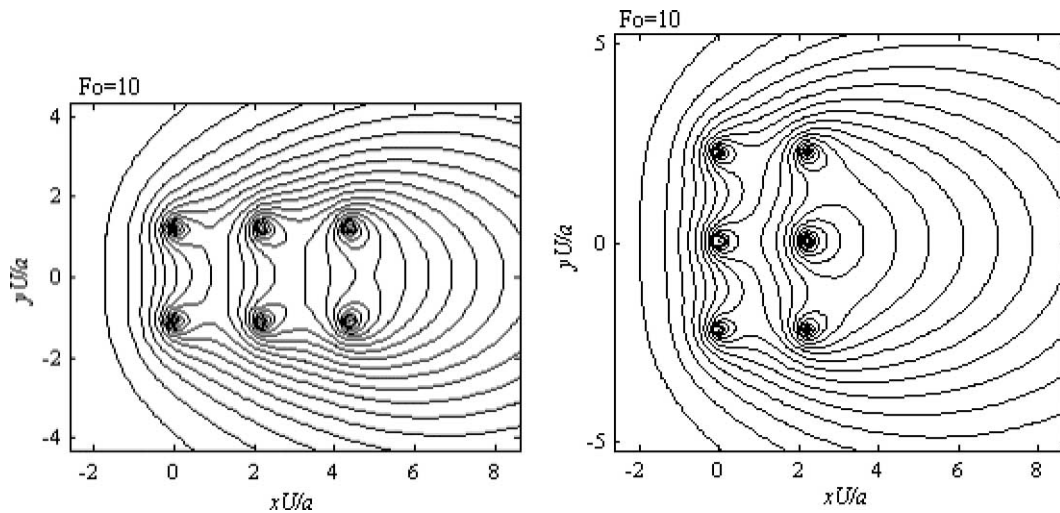


Fig. 7. Isotherms of a borehole field with different configurations to the advection direction.

a certain borehole wall can be obtained by summing up all the temperature excesses caused by individual U-tubes, i.e.,

$$\theta_m = \bar{\theta}(r_b, \tau) + \sum_{i=1}^{N-1} \theta(r_i, \varphi_i, \tau) \quad (15)$$

where  $r_i$  and  $\varphi_i$  denote the distance and polar angle between the  $i$ th borehole and the borehole concerned.

As an example, isotherms in a GHE field with  $2 \times 3$  boreholes are shown in Fig. 7. Two different borehole configurations are considered corresponding to the water advection direction. Different temperature distribution patterns are resulted in due to different interaction of the individual boreholes. Generally, the impacts of advection would be the most significant for a field that consisted of a single line of boreholes oriented perpendicular to the groundwater flow direction. Thus, it is recommended that the GHE field be oriented to minimize the number of boreholes in the thermal shadow of others if the groundwater flow direction is known and if the site configuration allows.

Moreover, variation in load and on-off cycling of the GHE can be considered by superimposition of a series of heating pulses [13]. Consequently, the temperature on the borehole wall can then be determined for any instant on specified operational conditions. In this way the analytical solution presented above can be integrated without difficulty into existing tools for design and simulation of GHEs in ground-coupled heat pump systems as long as adequate knowledge is available on the local hydrogeology.

#### 4. Discussion on practical geological conditions

While the analytical solutions presented above have laid a theoretical basis, it is critical also to know the groundwater flow in certain locations for assessing its impact on GHE performance. The non-dimensional distance and time,  $R =$

$\frac{r}{L} = \frac{u\rho_w c_w r}{k}$  and  $Fo = \frac{\tau}{T} = \frac{(u\rho_w c_w)^2 \tau}{k\rho c}$ , determine the deviation of the heat transfer regime under groundwater advection conditions from that of heat conduction alone. Both the parameters are strong functions of the groundwater flow rate. Of these non-dimensional parameters,  $R$  plays an even more decisive role. As indicated by the solutions, heat transfer of this problem is dependent on the flow velocity and the thermal properties of the medium. Meanwhile, the groundwater flow is determined by both the local hydraulic gradient and the hydraulic conductivity of the geologic formations. The groundwater flow rate and the thermal properties of soils and rocks encountered in GCHP practices cover substantially wide ranges. Values of hydraulic gradient are somewhat more site-specific. The United States Environmental Protection Agency reports a typical range of hydraulic gradient values of 0.0001–0.05 [10]. Some of typical values of the hydraulic and thermal properties of soils and rocks may be found in literature. The data summarized by Chiasson et al. [10] have been adapted and listed in Table 1 for the purpose of presenting a rough sense on the order of magnitude of the influencing factors of various geological formations. In the problem of a line source in an infinite medium defined above, no specific geometric size exists which may serve as a representative length. For engineering applications a certain linear dimension,  $L_c$ , such as the borehole radius, the spacing between the boreholes [10], the length of the borehole field in the direction of flow, or even the mean grain size of the porous medium [14] can be chosen as a representative size of the problem. In this case the non-dimensional parameter  $R_c = u\rho_w c_w L_c / k$  may be defined as the Peclet number,  $Pe$ , in some studies, and serve as a measure of the relative advection intensity. Because the value of the Peclet number is dependent on the representative length chosen, it is inconvenient to compare among data from different studies. Here we list in Table 1 only the characteristic size  $L$  and time  $T$  in the problem. According to the listed data the non-dimensional parameter  $R$  or  $Pe$  can be determined readily once a representative length is chosen, and quantitative

Table 1

Typical values of hydraulic and thermal properties of soils and rocks and their characteristic length and time in conduction–advection heat transfer

| Medium                              | $K$<br>[m·s <sup>-1</sup> ] | $\varepsilon$ | $u^*$<br>[m·s <sup>-1</sup> (m·yr <sup>-1</sup> )] | $k^{**}$<br>[W·m <sup>-1</sup> ·K <sup>-1</sup> ] | $\rho c$<br>[J·m <sup>-3</sup> ·K <sup>-1</sup> ] | $L = \frac{k}{u\rho_w c_w}$<br>[m] | $T = \frac{k\rho c}{(u\rho_w c_w)^2}$<br>[s (yr)] |
|-------------------------------------|-----------------------------|---------------|--|---|---|------------------------------------|---|
| Gravel                              | 3.0E-3                      | 0.31          | 3.0E-5<br>(946)                                    | 0.98  | 1.4E+6  | 7.80E-3                            | 87<br>(2.76E-6)                                   |
| Sand (coarse)                       | 7.3E-5                      | 0.385         | 7.3E-7<br>(23.0)                                   | 1.02  | 1.4E+6  | 0.334                              | 1.53E+5<br>(4.85E-3)                              |
| Sand (fine)                         | 6.3E-6                      | 0.40          | 6.3E-8<br>(1.99)                                   | 1.03  | 1.4E+6  | 3.90                               | 2.07E+7<br>(0.656)                                |
| Silt                                | 1.4E-7                      | 0.475         | 1.4E-9<br>(4.42E-2)                                | 2.07  | 2.85E+6   | 353                                | 1.72E+11<br>(5.45E+3)                             |
| Clay                                | 2.2E-10                     | 0.47          | 2.2E-12<br>(6.94E-5)                               | 1.25  | 3.3E+6  | 1.36E+5                            | 4.86E+16<br>(1.54E+9)                             |
| Limestone, dolomite                 | 7.7E-8                      | 0.10          | 7.7E-10<br>(2.43E-2)                               | 2.46  | 1.34E+7   | 763                                | 3.17E+12<br>(1.01E+5)                             |
| Karst limestone                     | 1.0E-4                      | 0.275         | 1.0E-6<br>(31.5)                                   | 3.56  | 1.34E+7   | 0.850                              | 2.72E+6<br>(8.60E-2)                              |
| Sandstone                           | 4.2E-8                      | 0.18          | 4.2E-10<br>(1.32E-2)                               | 4.50  | 3.56E+6   | 2.56E+3                            | 5.18E+12<br>(1.64E+5)                             |
| Shale                               | 1.4E-11                     | 0.0525        | 1.4E-13<br>(4.42E-6)                               | 2.53  | 3.94E+6   | 4.32E+6                            | 2.90E+19<br>(9.20E+11)                            |
| Fractured igneous and metamorphic   | 1.5E-6                      | 0.05          | 1.5E-8<br>(0.473)                                  | 4.61  | 2.20E+6   | 73.4                               | 2.57E+9<br>(81.5)                                 |
| Unfractured igneous and metamorphic | 2.4E-12                     | 0.025         | 2.4E-14<br>(7.57E-7)                               | 4.59  | 2.20E+6   | 4.57E+7                            | 1.0E+21<br>(3.17E+13)                             |

\* Based on an assumed hydraulic gradient of 0.01 m·m<sup>-1</sup>.

\*\* Saturated with water.

comparison can be carried out on the basis of the solutions presented.

The data in Table 1 show that the hydraulic conductivity, and then, the advection velocity in the case of identical hydraulic gradient, of the gravel and coarse sand are the highest among the various geological formations. It decreases by four orders of magnitude as matrix particle sizes decrease to silts and a further three orders of magnitude for clays. Being inversely proportional to the advection velocity, the characteristic size of the advection process varies dramatically as well for different formations. On the other hand, the characteristic time is inversely proportional to the square of advection velocity, and then covers an even broader range from a few minutes to 10<sup>13</sup> years as indicated in the table. Therefore adequate understanding of local geology and groundwater flow is of great importance to estimate the effects of groundwater flow on GHE performance. Combined with discussions in the foregoing sections, the data in Table 1 suggest that the effects of groundwater flow may usually be neglected except in formations with considerable flow rate such as gravel and coarse sand.

## 5. Conclusion

The analytical solution, Eq. (8), has been derived of the temperature response around a line source in an infinite porous medium with uniform water advection. The non-dimensional correlation, Eq. (11), reveals that the nor-

malized temperature rise is a function of non-dimensional coordinates and time only. Compared with the conventional Kelvin's line-source model, which makes no account of the water advection, this solution indicates that the impact of moderate groundwater flow on the heat transfer process may be prominent. The actual magnitude of the impact, however, depends mainly on the flow rate, which is characterized by the non-dimensional parameter  $R$ . This explicit and concise expression can provide an appropriate footing for qualitative and quantitative analysis of this impact for vertical ground heat exchangers in GCHP systems.

The mean temperature on a circle around the line source is also derived as a simple function of the radial distance and time, which is significant in determining the temperature on borehole walls for GHE applications. It is noticeable that the ratio of the temperature rises at certain locations of the same distance from the source is independent of time.

The duration for the temperature distribution to approach its steady state under the condition of constant heating rate has great implications in considering the effect of groundwater flow. The solution has revealed that the characteristic time  $T = \frac{k\rho c}{(u\rho_w c_w)^2}$  and corresponding non-dimensional time  $Fo = \frac{r}{T}$  are also a decisive factor for the transient process.

By means of the superimposition principle this analytical solution can be employed readily in determining the temperature rise in a borehole field with variable heating rates, and then, integrated into existing software for GHE design and simulation.



Finally, although a rough summary of the thermal and hydraulic properties of various soils and rocks is presented in this paper, proper assessment of the impact of water advection is often hindered in engineering practice by lack of sufficient information on groundwater flow. Most GHE designers have not generally found it feasible or cost-effective to obtain the hydrological data required for the assessment. Consequently, more efforts should be made in understanding the implications of practical geological and hydraulic conditions in engineering practices.

## References

- [1] J.E. Bose, M.D. Smith, J.D. Spitler, Advances in ground source heat pump systems—an international overview, in: Proceedings of the Seventh International Energy Agency Heat Pump Conference, China Architecture & Building Press, Beijing, 2002, pp. 313–324.
- [2] S.P. Kavanaugh, K. Rafferty, Ground Source Heat Pumps—Design of Geothermal Systems for Commercial and Institutional Buildings, American Society of Heating, Refrigerating and Air-Conditioning Engineers (ASHRAE), Atlanta, 1997.
- [3] L.R. Ingersoll, O.J. Zobel, A.C. Ingersoll, Heat Conduction with Engineering, Geological and Other Applications, McGraw-Hill, New York, 1954.
- [4] J.E. Bose, J.D. Parker, F.C. McQuiston, Design/Data Manual for Closed-Loop Ground Coupled Heat Pump Systems, Oklahoma State University for ASHRAE, Stillwater, 1985.
- [5] Caneta Research Inc., Commercial/Institutional Ground Source Heat Pump Engineering Manual, American Society of Heating, Refrigerating and Air-Conditioning Engineers (ASHRAE), Atlanta, 1995.
- [6] H. Zeng, N. Diao, Z. Fang, A finite line-source model for boreholes in geothermal heat exchangers, Heat Transfer Asian Res. 31 (2002) 558–567.
- [7] H. Zeng, N. Diao, Z. Fang, Heat Transfer Analysis of boreholes in vertical ground heat exchangers, Internat. J. Heat Mass Transfer 46 (2003) 4467–4481.
- [8] P. Eskilson, Thermal analysis of heat extraction boreholes, Doctoral Thesis, Department of mathematical Physics, University of Lund, Lund, Sweden, 1987.
- [9] H.S. Carslaw, J.C. Jaeger, Conduction of Heat in Solids, second ed., Oxford Press, Oxford, 1959.
- [10] A.D. Chiasson, S.J. Rees, J.D. Spitler, A preliminary assessment of the effects of groundwater flow on closed-loop ground-source heat pump systems, ASHRAE Trans. 106 (2000) 380–393.
- [11] E.R.G. Eckert, R.M. Drake, Analysis of Heat and Mass Transfer, McGraw-Hill, New York, 1972.
- [12] N. Diao, Q. Li, Z. Fang, An analytical solution of the temperature response in geothermal heat exchangers with groundwater advection, J. Shandong Inst. Archit. Engng. 18 (3) (2003) 1–5.
- [13] Z. Fang, N. Diao, P. Cui, Discontinuous operation of geothermal heat exchangers, Tsinghua Sci. Technol. 7 (2) (2002) 194–197.
- [14] J. Bear, Dynamics of Fluids in Porous Media, Dover, New York, 1972.